NUMERICAL SIMULATION OF PLANING HULL IN REGULAR WAVES

TANVIR MEHEDI SAYEED

NUMERICAL SIMULATION OF PLANING HULL IN REGULAR WAVES

by

Tanvir Mehedi Sayeed

A thesis submitted to the School of Graduate Studies

in partial fulfillment of the requirement for the

degree of Master of Engineering

Faculty of Engineering and Applied Science

Memorial University of Newfoundland

August 20, 2010

St. John's, Newfoundland, Canada

Abstract

The problem of predicting the motions of planing craft is extremely difficult. The planing hull motions in waves lead to strong non-linearities that cannot be depicted well by linear analysis of motion. A non-linear mathematical model (3 degree of freedom program) has been developed for predicting the vertical motions of a planing hull in regular head waves. Since the model is non-linear, the computations are made in the time domain. The model has its origins in the non-linear strip theory developed by Zarnick (1978). The model can input variable deadrise angles to account for hull geometry. It is assumed that the wavelengths are large in comparison to the boat length and the wave slopes are small. Wave input is restricted to monochromatic linear deep water waves. The thrust and the friction drag forces are assumed to act through the centre of gravity. The hull is divided into a series of two-dimensional wedges. The forces and moments acting on the craft are calculated by modelling wedge impact and integrating the result along the length of the hull. This model can also predict the vertical accelerations which are important design criteria for planing hulls.

The numerical model is verified with the experimental model test results of Fridsma (1969), Chiu & Fujino (1989), and Katayama et al. (2000). The model has shown promising results in predicting the heave and pitch motions in semi-planing and planing regions of speed. For the very high speed vessels and to predict the vertical accelerations, the model still needs to include exact slamming forces.

Experimental investigations have been carried out with a $10°$ deadrise wedge varying the drop heights and the mass of the wedge. These factors have been found to have negligible influence in predicting the maximum pressure coefficient. The analytical prediction method developed by Chuang (1973) is found to be an accurate tool for determining maximum slamming pressures. Follow up experiments could be performed varying the deadrise of the wedge and doing some oblique drop tests to further verify Chuang's (1973) prediction method. Then this method could be implemented in the numerical simulation of planing hulls.

Acknowledgements

I would like to express my sincere gratitude and indebtedness to my supervisors Dr. Heather Peng and Dr. Brian Veitch for their careful supervision, restless encouragement, invaluable suggestions, untiring assistance, and benevolent support throughout the development of this thesis. Dr. Peng has continually given me valuable advice on my thesis work and always kindly helped me to overcome difficulties.

I also appreciate the support of the Natural Sciences and Engineering Research Council of Canada (NSERC), the Virtual Marine Technology (VMT), the Mathematics of Information Technology and Complex Systems (MITACS), and the Graduate Fellowship from Memorial University of Newfoundland. This work would not have been completed without their financial support.

Sincere thanks and gratitude are extended to professors in Engineering for courses they offered and to my fellow graduate students for friendship and pleasant memories we shared in the last two years. Finally, I am profoundly grateful to my parents and rest of my family members for their love, support, and encouragement.

Table of Contents

List of Figures

List of Tables

Nomenclature

$[A]$	Mass matrix
a_{BF}	Buoyancy correction factor
a_{BM}	Moment correction factor
b	Half beam
B	Beam of craft, $2b$
c	Wave celerity
C_v	Beam Froude number, $V/\sqrt{gB}$
C_D	Cross flow drag coefficient
d	Depth of penetration of each section
D	Friction drag
$\vec{F}$	Force vector which is a function of state variables
f_B	Sectional buoyancy force
f_{CD}	Sectional hydrodynamic lift due to the cross flow drag
f_M	Sectional hydrodynamic lift due to the change of fluid momentum
Fn	Froude number, $V/\sqrt{gL}$
F_x	Hydrodynamic force in x direction
F_y	Hydrodynamic force in y direction
F_θ	Hydrodynamic moment about pitch axis

g	Acceleration due to gravity
H_w	Wave height
I	Pitch moment of inertia
I_a	Added pitch moment of inertia
k	Wave number
k_a	Added mass coefficient
l	Wetted length of the craft
L	Length of planing craft
LCG	Longitudinal centre of Gravity
m_a	Sectional added mass
M	Mass of planing craft
M_a	Added mass of craft
N	Hydrodynamic normal force
p_i	Impact pressure
p_p	Planing pressure
p_t	Total pressure, $p_i + p_p$
T_x	Thrust component in x direction
T_z	Thrust component in z direction
U	Craft velocity parallel to keel
V	Craft velocity perpendicular to keel
V_n	Relative normal velocity of the impact body to the wave surface

V_v	Vertical impact velocity
VCG	Vertical center of gravity
w	Sectional weight of craft
W	Weight of craft
w_z	Wave orbital velocity in vertical direction
$\vec{x}$	State variable vector
x_c	Distance from center of gravity to center of pressure for normal force
x_d	Distance from center of gravity to center of action for friction drag
x_p	Moment arm of thrust about center of gravity
$x_{CG}, \dot{x}_{CG}, \ddot{x}_{CG}$	Surge displacement, velocity and acceleration
$z_{CG}, \dot{z}_{CG}, \ddot{z}_{CG}$	Heave displacement, velocity and acceleration
$\theta, \dot{\theta}, \ddot{\theta}$	Pitch angle, velocity and acceleration
x, y, z	Global coordinate system
ξ, χ, ζ	Body coordinate system
η	Wave elevation
η_0	Wave amplitude
β	Deadrise angle
ν	Wave slope
λ	Wave length
ρ	Density of water

Chapter 1

Introduction

Seakeeping performance is one of the major concerns of a ship or floating structure subjected to waves. Naval architects strive to achieve seaworthiness in adverse and rough sea environments. The seakeeping analysis of the high speed planing hulls is more complex because such vessels exhibit strong non-linearities when operating in a seaway.

1.1 Planing Hull versus Displacement Hull

The shape of the hull is an important factor in determining a ship's performance in calm water and in waves. Displacement hull and planing hull are two of the basic hull types. Other hull configurations combine features of the displacement and planing hulls and are called semi-displacement or semi-planing.

Displacement ships are generally slower than planing crafts. They are predominantly supported by the weight of the water they displace (hydrostatic buoyancy force). As speed increases, displacement hulls push through the water without generating hydrodynamic lift. Normally these vessels are restricted in their speed.

Planing crafts are high speed vessels with beam Froude numbers greater than one. A planing boat runs skimming across the water surface by developing dynamic lift at its bottom, greatly reducing skin friction and wave making resistance [Payne (1988)]. The planing hull weight is predominantly supported by hydrodynamic lift and the area of the submerged portion is small compared with displacement hulls. Planing hulls usually have a shallow V-bottom with at least one chine. Such configuration helps these vessels to produce required hydrodynamic lift to reach the planing mode.

Most of the recreational boats and jet-skis are of semi-planing or planing type. Such vessels are widely used in military such as fast rescue craft (FRC), patrol boats, and rapid response craft. They also have their commercial applications such as pilot craft, tenders, inshore lifeboats, and offshore supply operation for oil industry.

1.2 Non-linearities associated with Planing Hull

The high speed planing crafts in waves exhibit significant non-linearities. A brief description of the factors causing strong non-linearities in planing hull is presented in the following section.

- **Effect of Forward Speed**

The non-linear behavior is small at low speed but increases considerably with increasing forward speed [Fridsma (1969)]. With an increase in forward speed, the hull's wetted surface is greatly reduced, thus reducing the buoyancy lift and increasing the hydrodynamic lift. The sinkage and trim also become significant at high forward speed, which causes reduction of wetted surface and submerged volume. This, in turn, would cause a reduction of the frictional and wave making resistance. This is the basic concept of planing hull design. Keuning (1994) discussed some of the results of Clement and Blount (1963) and concluded that the absolute magnitude of the sinkage and trim varies considerably with increasing speed. Fridsma (1969) also found greater added resistance at longer wavelengths at high forward speeds.

- **Effect of Sinkage and Trim**

The isolated effect of either sinkage or trim, keeping all other design parameters constant, is physically not possible to investigate. Fridsma (1969) showed the influence of trim on heave and pitch motions and vertical accelerations at the centre of gravity and at the bow. From his results, it is evident that the effect of trim is significant at high forward speed, especially on the vertical accelerations.

The vertical accelerations are very important parameters for the prediction of the operability of planing crafts in waves. Keuning (1994) mentioned that a computational model excluding sinkage and trim is not justifiable for the predictions of planing craft motions in waves.

- **Effect of Deadrise**

The effect of deadrise is also an important factor in the design criteria of planing hull. As speed increases, this effect becomes more significant. The high deadrise hull sits deeper in the water with less trim. This reduction in trim will decrease the motions and accelerations [Keuning (1994)]. The experimental results of Fridsma (1969) show that the heave and pitch motions are drastically reduced with increasing deadrise at high speed-length ratios. The resonant motions become smaller and the tendency of the boat to fly and leave the water surface is reduced with higher deadrise. At high speed-length ratios the sharply tuned resonant peaks in the motion and acceleration responses prohibit practical operations, particularly for low deadrise boats.

- **Large Relative Motions**

Resonance occurs when the natural frequency of the motion is the same as the encounter frequency of the waves. When the planing craft moves at high forward speeds in waves, resonance occurs at relatively longer and larger waves, which results in large relative motions. These effects associated with the large relative motions and the change in wetted surface along the length should be considered to get an accurate prediction of motions.

1.3 Objectives of Study

Simulation training is widely used in the aircraft industry to train pilots to operate aircraft. Likewise, ship bridge simulators are used to train the crews of large vessels. The efficacy of this type of training is recognized by international standards and is often required by regulations. A new application of simulation training technology is being developed by Virtual Marine Technology (VMT) in co-operation with researchers at Memorial University of Newfoundland. Specifically, they have developed immersive training simulators for small vessels, such as lifeboats and fast rescue craft. The simulated environment is ideal for exposing trainees to safety critical and dangerous operations –

which are common in lifeboat evacuations and fast rescue craft operations. To be effective, the simulated environment must represent reality with a high degree of fidelity. This requires accurate mathematical models of complex phenomena, such as vessel motions in a seaway. The present research deals with the modeling of planing hulls in regular waves that could be extended for irregular sea. I will then incorporate this in a simulation environment where it will improve the training provided to mariners. Ultimately, it should improve the safety of life at sea.

1.4 Thesis outline

The present thesis is divided into five chapters. Chapter 1 presents a preliminary introduction of planing hull and non-linearities involved with the motions of planing hull. In Chapter 2, a brief literature review relating to wedge impact, motion analysis of planing hull by strip theory, and other approaches and some significant experimental research works are presented. Chapter 3 discusses the mathematical formulation and the numerical approaches that have been applied to solve the motion equations in the time domain. Chapter 4 presents the validation and verification of the numerical results with the experimental model test results of Fridsma (1969), Chiu & Fujino (1989), and Katayama et al. (2000). Summary and conclusions as well as recommendations for future work are presented in Chapter 5.

Chapter 2

Literature Review

The study of the hydrodynamic behavior of planing crafts in waves by many researchers shows considerable diversity in their approaches. A brief discussion of these various modeling schemes is presented in this chapter.

2.1 Previous Research Relating to Wedge Impact

The study of planing craft is closely related to the study of the fundamental water impact situation where a two-dimensional wedge penetrates a calm water surface.

The first attempt to model loads on a planing hull was made by Von Kármán in 1929 with his pioneering studies of loads on seaplane floats. The advent of hydroplanes led to increasing interest in calculations of the forces on their bottom while landing. Von Kármán reduced the 3-D problem to a 2-D and simplified the cross section of floats of sea-planes to a wedge. According to Von Kármán's momentum theory, when a body enters the water its original momentum is distributed between the body and the surrounding water. The forces acting on the body can be evaluated by the rate of change of momentum. He also approximated the added mass of a wedge shaped body as that of a flat plate with same length and width. Therefore, for a certain immersion the added mass of the wedge is equal to the mass of water contained in a semi cylinder having a length equal to the length of the wedge and a diameter equal to the wetted width of the wedge at that immersion. Von Karman's work was applied to the maximal pressure estimation on the floats of hydroplanes during sea landings.

A similar study of two-dimensional water impact on solid bodies was conducted by Von Herbert Wagner (1932). Instead of considering a wedge, Wagner reduced the problem to dropping a plate on the water surface, considering that the virtual plate width varies over time. There is good agreement between the Wagner and the Von Kármán formulae in the particular case of a wedge entering water. Water rise or splash-up was not considered by Von Kármán but Wagner took this into account reducing the problem to dropping a plate and assuming that the virtual plate width varies with time.

Payne (1981) claimed the original Von Kármán's theory as superior than other later refinements. Payne (1981) presented a model to calculate maximum pressure away from the keel, which is an improvement on Von Kármán's theory. Payne also validated his prediction model with available pressure data from Chuang's (1967) experiments and found the model to be in reasonable agreement.

S.L. Chuang (1973, 1976) developed a prediction method for determining slamming pressures of a high speed vessel in waves. This method is based on the Wagner wedge impact theory, the Chuang cone impact theory [Chuang (1969)], and NSRDC drop tests of wedges and cones. Then Chuang conducted some slamming tests of three dimensional models in calm water and in waves. The experimental results matched quite accurately with the predicted results.

Zhao et al. (1996) presented a fully non-linear boundary element method and another approximate method based on the extension of Wagner's solution to solve the water entry problem. The boundary element method included flow separation and the extension of Wagner's solution did not include flow separation. The numerical results were verified with the experimental drop tests of a wedge and a bow flare section.

Wu et al. (2004) analyzed a 2-D wedge in free fall motion based on velocity potential theory ignoring the gravity effect. They compared the similarity solution and time domain solution with experimental drop test results.

Peseux et al. (2003) used the finite element method to solve the highly non-linear hydrodynamic impact problem. They performed the numerical analysis for both rigid and deformable structures. A series of drop tests were also conducted on rigid and deformable cone-shaped structures to validate the numerical results.

2.2 Numerical Works Based on Strip Theory

Martin (1978a) studied the coupled heave and pitch instability of planing crafts in calm water, called porpoising. He developed a method for predicting the conditions that lead to porpoising in the surge, pitch, and heave directions for prismatic hulls. The same linear equations of motions were later used by him to model the heave and pitch response to regular waves, Martin (1978b). The linear model showed promising results for determining the effects of various parameters such as trim angle, deadrise, loading, and speed on the damping, natural frequency, and linearized response in waves. However, Martin concluded that the linear frequency domain model could not reproduce accelerations accurately and the accurate prediction of large motions and peak accelerations requires a non-linear analysis.

Martin suggested a time-domain analysis, which was presented the same year by Zarnick (1978). The Zarnick model became the basis of most of the later developed simulation codes including FASTSHIP by Keuning (1994), BOAT3D by Payne (1995), and POWERSEA by Akers (1999).

E.E. Zarnick (1978), following the work of Martin, developed a nonlinear mathematical model using low aspect ratio strip theory for a V-shaped prismatic body with hard chines having a constant deadrise angle planing at high speed in regular head waves. It was assumed that the wavelengths were large in comparison to the boat length and the wave slopes were small. Wave input was restricted to monochromatic linear deep water waves. In the simplified problem, Zarnick assumed that the craft was towed at constant speed and the thrust and the friction drag forces were assumed to act through the centre of gravity. The coefficients in the equation of motion were determined by a combination of theoretical and empirical relationships. The hull was divided into a series of 2-D wedges. The forces and moments acting on the craft were calculated by modelling wedge impact and integrating the result along the length of the hull. This model can also predict the vertical accelerations, which are an important consideration in designing a planing craft. Computed heave and pitch motions and phase angles as well as bow and centre of gravity accelerations, were compared with the experimental results of Fridsma (1969).

Chiu and Fujino (1989) included an elastic parameter to Zarnick's (1978) theory by considering the inertial effects. They ignored the second and higher order terms in the equations of motion and also ignored the cross-flow drag associated with three-dimensional effects acting on low aspect ratio bodies. The sectional hydrodynamic coefficients were evaluated at an encounter frequency for the oscillatory motion and at infinite frequency for the steady forward motion. They also conducted some model tests with a simplified ship model of a hard chine type and a ship model of a round bilge type. They verified their numerical prediction model with those model test results and the results of Fridsma (1969). They also explained the huge sagging moment that occurs at the midship of a planing craft travelling at high speed in head seas.

Keuning (1994) extended Zarnick's (1978) model to incorporate a formulation for the sinkage and trim of the ship at high speeds. He also studied the hydrodynamic lift distribution along the length of the ship with non-linear added mass and wave exciting forces in both regular and irregular waves. He added a semi-empirical tool for estimating the calm water running attitude in order to determine correction factors to the dynamic simulation procedure. Keuning (1994) validated his computational model with model test results carried out with the three parent models of the Delft Systematic Deadrise Series having 12.5, 25, and the 30 degrees deadrise, respectively. He used those model test results and some of the results of Fridsma (1969) to check the capability of the computational model to predict non-linear behavior. He also concluded that using linear computational models for the prediction of the operability of fast monohulls in waves may lead to erroneous results. He suggested a computational model including the important non-linear effects that can predict the motions in waves with higher accuracy.

Hicks et al. (1995) expanded the full nonlinear force and moment equations of Zarnick (1978) in a multi-variable Taylor series. They replaced the equations of motion by a set of highly coupled, ordinary differential equations with constant coefficients, valid through third order. This expansion of the fluid forces can predict the linear stability boundaries. They also identified the areas of critical dynamic response and the influence of selected second order terms on porpoising.

Richard H. Akers (1999) summarized the semi-empirical method, three-dimensional panel method, and their advantages and drawbacks dealing with planing hull motion analysis. He reviewed in detail the two-dimensional low aspect ratio strip theory developed by Zarnick (1978). Akers modeled the added mass coefficients based on an empirical formula that is a function of deadrise angle. The simulation results were validated with model test results of Fridsma (1969, 1971) for both regular and irregular seas. The buoyancy and moment coefficients were adjusted to match Fridsma's (1969) calm water resistance and trim. The algorithm predicted heave and pitch motion and added resistance quite accurately, but the predicted accelerations were less accurate. The theory was extended to predict hull panel pressures in irregular seas and the results matched quite well with those calculated using Spencer's (1975) method.

A thorough investigation of the vertical plane motions of a planing craft operating in calm water and in waves has been made by Blake (2000). He presented a frequency domain linear model based upon Martin (1978a, 1978b) and found that the inclusion of time-dependent wetted lengths is required to improve the prediction of the craft performance. Then he presented a time domain non-linear model and also investigated the frequency dependency of added mass and damping terms. The influence of the variation of various design parameters is also illustrated. One configuration based on Fridsma's (1969) 30^0 deadrise (configuration K) was constructed and tested in calm water and regular waves to further justify Fridsma's (1969) results and validate the theory. The variation of the wetted length of the craft was also measured with the help of a computer vision data acquisition (CVDA) system. The performance of planing craft in irregular seas was investigated using an ITTC78 spectrum. He also concluded that the linear frequency domain approach is useful in quantifying stability boundaries and the non-linear strip theory approach allows accurate quantification of planing craft responses in the vertical plane.

Grame et al. (2003) presented a similar time-domain analysis of simulating a planing hull in head seas, which is different from the classical Zarnick's model in pre-calculation scheme of hydrostatic and hydrodynamic coefficients. He applied pre-calculated cross-section data to achieve better hull geometry. The complete load distribution in his model is determined before integration to the rigid body equations of motion.

Later, Grame (2005) improved his model by adding a reduction function based on model tests and published model data for the near-transom pressure, and this reduced the pressure near the stern gradually to zero at the stern. This approach improved the simulation of the planing hull in calm water and in head waves for medium and high speed configurations with the beam Froude numbers, C_v greater than 2.

Lewis et al. (2006) also described the numerical model developed by Blake (2000), which also has its origins in the non-linear strip theory developed by Zarnick (1978). They validated the model at higher speeds using model test data from two scale models: A wave piercing rigid inflatable boat (RIB) and an Atlantic 21 RIB. The experiments were conducted in a range of regular wave frequencies for three wave heights together with a realistic JONSWAP sea spectrum. They found the numerical model predicted the motions of the craft with larger magnitude and suggested a few possibilities to improve the accuracy of the model.

van Dayzen (2008) extended the original model developed by Zarnick (1978) and later extended by Keuning (1994) to three degrees of freedom: surge, heave, and pitch motion in both regular and irregular head seas. The simulations can be carried out with either a constant forward speed or constant thrust. He also validated the results with experimental data of two models, a conventional double chined planing monohull (DCH) and a modern axebow (Axehull). He found his model very sensitive to hull geometry and suggested that a thorough investigation of hydrodynamic coefficients has to be carried out in order to get a more accurate computational model.

2.3 Numerical Work Based on Other Approaches

Lai and Troesch (1995) used a three-dimensional planing theory that incorporates vortex lattice methods (VLM) to determine hydrodynamic forces and moments in calm water at high speeds. A model was developed taking into account the issues associated with planing such as slenderness, linearity of boundary conditions, wetted surface contours, jet development, and panel shape. They also examined the model including the effect of gravity in the near field.

The numerical details of the model as formulated in terms of the vorticity distribution are presented in Lai and Troesch (1996). The vortex lattice panels are distributed in the computational surface of the hull and the jet region. The body boundary conditions are satisfied at the control points that are located at the centroid of each panel. To solve the boundary value problem, the body boundary condition, free surface boundary condition, velocity continuity on the chine, and Kutta condition for the trailing edge have been satisfied. In addition to common characteristics of VLMs, three special features have been implemented in their vortex lattice model: overlap panels that all start from the keel are used, subpanels with linear strength inside each regular panel are added, and the vorticity strength in the x-direction for each panel is treated as an unknown.

Zhao et al. (1997) demonstrated hydrodynamic analysis of planing craft in calm water using a $2.5D(2D+t)$ approach, which means a two-dimensional Laplace equation with three-dimensional free-surface conditions. They also included the flow separation from chines or spray rails. The method based on potential theory can predict calm water resistance, sinkage, and trim due to pressure effects. The results were also verified with experimental drop test results of a wedge and a bow flare section with knuckles. Faltinsen (2005) has provided details of this approach in his textbook.

Caponnetto et al. (2003) presented three different methods for simulating planing boats in waves. One is based on the extension of Wagner's theory (1932) and the other two methods are based on the computational fluid dynamics solver COMET, using the Reynolds Averaged Navier Stokes equations (RANSE). For using the solver COMET, they applied a finite-volume method. The free surface was accounted for by a volume-of-fluid (VOF) method and turbulence was approximated using $k-\in$ model. They also validated their simulation results with some of the experimental results of Katayama et al. (2000) and found that simulations using COMET show better agreements with experimental results. They achieved the steady state solution for regular waves after about 33 hours CPU time and this approach for irregular waves was out of scope. They also concluded that non-linear simulations are the appropriate tool for predicting the motions of planing crafts in waves.

Ghassemi and Yu-min (2008) determined the hydrodynamic forces of a planing hull using potential based boundary element method (BEM) including boundary layer effects.

In order to calculate the induced resistance and lift, boundary conditions were satisfied on the body surface, on the free surface, at the stern end, and at infinity. A boundary layer analysis based on the calculations of the momentum integral equations was employed to determine the frictional resistance. Finally, an empirical tool based on Savitsky (1964) was applied in the region of upwash geometry to determine spray resistance. Their combined method predicted well the pressure distribution of the hull surface and it predicted that the hydrodynamic lift to weight ratio is about 65% and 85% at length based Froude numbers, $Fn = 3.35$ and $Fn = 5.0$, respectively.

Another approach is the finite pressure element method (FPEM). It was first applied by Doctors (1975) to the three-dimensional flat plates and prismatic hulls. The craft hull was modeled by the equivalent rectangular pyramidal pressure elements. The double integral equation in the Green function was simplified to a single integral by the use of a special function.

2.4 Experimental Works

Clement and Blount (1963) carried out a comprehensive set of model tests on a systematic series (TMB Series-62). In their experiments, they used a parent model with a deadrise of 12.5 degrees having a prismatic aftbody and varied the aspect ratio (length to beam over the chine), the loading (weight related to chine area) of the lifting surface and the longitudinal position of the centre of gravity. The models were run in calm water and the resistance, running trim, sinkage, and porpoising characteristics were investigated.

They found that the sinkage and trim were dependent on hull geometry, forward speed and the longitudinal position of the centre of gravity.

A notable contribution on the hydrodynamics of planing hull has been made by Savitsky (1964). He made a thorough investigation and developed a set of empirical planing equations for the lift, drag, wetted area, center of pressure, and porpoising stability limits of planing surfaces depending on speed, trim, deadrise and loading based his experimental data.

Savitsky (1968) categorized the rough-water performance of planing hulls into two speed regimes: speed-length ratios less than 2.5 and speed-length ratios greater than 2.5. In the first regime, the hulls can be classified as "semi-displacement". These hulls have seakeeping characteristics similar to displacement ships and the buoyant forces are dominant compared to dynamic lifting forces. He found in the other regime, the dynamic planing lift forces predominate and the hull behavior is very much different from the displacement ship. Also the hull impact force is the most limiting factor in this region.

Savitsky & Brown (1976), a continuation of the work of Savitsky (1964), presented semi-empirical procedures for running attitude, power requirements and porpoising stability based on collected data of experimental tests performed at the Davidson Laboratory at the Stevens Institute of Technology.

One of the first real drop tests with wedge-shaped models were conducted by Chuang (1967). The tests were performed with one rigid flat bottom model and five rigid wedges with deadrise angles of 1, 3, 6, 10 and 15 degrees respectively. The pressures were measured at the keel and away from the keel. The data from test results was used to provide a set of charts or empirical relations for estimating the maximum impact pressure due to rigid-body slamming of the wedges. It was concluded that the effect of trapped air needs to be taken in account for wedge angles between $0°$ and $3°$.

Engle & Lewis (2003) conducted experimental drop tests and made a comparison between experimental results and several numerical methods relating to the maximum water-impact pressure of a symmetrical wedge for different initial impact velocities.

Breder (2005) performed the drop tests to examine pressure loads on a rigid structure. He conducted the two-dimensional wedge drop tests with controlled vertical velocity, while earlier experiments involved the free fall water entry problem.

Peterson et al. (1997) reported some drop test results of a $20°$ deadrise prismatic hull model varying the drop height and weight and compared the results with a numerical water impact code.

Yettou et al. (2005) presented the results of experimental investigations of the pressure distribution on a free-falling wedge varying parameters such as drop height, the deadrise angle and the mass of the wedge. Existing models that assumed a constant water entry velocity of the wedge [Mei et al. (1999) and Zhao et al. (1996)] were compared with experimental data. Then they proposed a new model to predict the local maximum pressure based on the analysis of the experimental data.

A thorough experimental investigation of the constant velocity water entry problem has been performed recently by Tveitnes et al. (2008). They provided some useful information relating to wetting factor, flow momentum drag and added mass based on those experimental data analysis.

There is limited work available for planing craft in waves. Fridsma (1969) carried out experiments on a series of constant deadrise models in smooth water and regular head waves to define the effects of deadrise, trim, loading, speed, and length-to-beam ratio as well as wave proportions on added resistance, heave and pitch motions and impact accelerations. He found that the planing hull behaves much like a displacement ship at a speed-length ratio of 2 with the buoyancy forces playing the major role. The boat began to plane at a speed-length ratio of 4 in which condition the dynamic and buoyant forces are both significant. The hull was fully planing at a speed-length ratio of 6 in which condition the buoyancy plays only a minor role. The added resistance, motion response, and accelerations were found to be non-linear functions of the wave height except at a speed-length ratio of 2. At high speed-length ratios the sharply tuned resonant peaks in the motion and acceleration responses proved speed as a limiting factor in the design of rough water planing craft. Another important parameter was found to be the deadrise. At high speeds the motions and accelerations became drastically reduced with increasing deadrise. Trim also was found as a significant factor at high speeds. The results of Fridsma (1969) have been used by many researchers over the years: Martin (1978b), Zarnick (1978), Chiu & Fujino (1989), Keuning (1994), Akers (1999), Blake (2000), Grame et al. (2003) and Singleton (2008).

Akers et al. (1999) used experimental results of a full-scale high speed craft to verify the simulation results. A 7.62 m, 2903 kg, utility boat with twin outboard engines was used as a test boat to collect transient motion data. The boat was instrumented with two three axis accelerometers and a Watson inertial measurement unit. The testing was performed both in calm water and in the Kelvin diverging wake generated by a 12.954 m, 28 ton dive boat at 19 knots. The method was implemented in a computer program called POWERSEA including a simple wake model that can approximate the Kelvin diverging wake waves. After modeling and simulating the test boat in the POWERSEA program, they found that the simulation results predicted well the minimum and maximum accelerations at the sensor location in the hull, the pitch rate range and waveform shape, and the actual pitch position of the test boat.

Katayama et al. (2000) performed some model tests in calm water and regular waves at very high speed ranges (Fn =2.0 to 5.0). The motions were divided into some different types: linear motion, non-linear motion with and without jumping according to running conditions. They also compared their results with a simulation program developed using motion equations with experimental hydrodynamic coefficients and theoretical ones based on potential theory. From the results, they concluded that non-linear strip method with appropriately evaluated hydrodynamic forces can predict the vertical motions of a planing craft accurately enough for practical purpose.

Thornhill et al. (2001) presented a series of bare hull resistance test results performed in the Clearwater Towing Tank at the National Research Council of Canada's Institute for Ocean Technology with a 1/8 scale model of an 11.8 m long planing craft. A series of resistance tests were performed over a range of speeds and in 6 different ballast conditions. The tow force, running trim, sinkage, hull pressures, wetted surface areas and wave profiles were measured for those ballast conditions. The resistance and running trim results were found to show typical characteristics of planing hull identifying the 'hump' speed at which planing begins. The authors also identified the porpoising threshold for the model. Hull pressures were found to increase in the forward portion of the hull with increasing speed but decreased and became negative in the aft. The authors explained this by taking into account the potential head due to depth of immersion, which is usually omitted in simple classical planing theory. The boundary layer velocity profile below the hull surface was measured at the design ballast condition using a laser Doppler velocimeter (LDV). The boundary layer thicknesses were found to increase in the direction of flow and to decrease as the model speed increases.

Grame et al. (2003) performed model tests with a prismatic transparent model based on Fridsma's (1969) 30° deadrise model running in calm water and in regular waves at different speeds. The results were found to overestimate lift in the transom area. A full scale trial was also performed with the combat craft 90E at high speeds. Rigid body motions were measured in all six degrees of freedom in addition to vertical acceleration at the centre of gravity and at the bow. The trials were performed at several sea states with significant wave heights ranging from 0.4 to 1.5 m. The irregular sea states were modelled by Monte-Carlo simulation of a two-parameter ITTC78 spectrum. The simulated results agreed very well for heave motion, vertical velocity and acceleration, but overestimated pitch motion.

Chapter 3

Computational Model

From the previous studies and experimental results it is evident that planing hull motion in waves lead to strong non-linearities which cannot be depicted well by linear analysis of motion. This chapter describes the non-linear mathematical model that is addressed to solve the equations of motion in the time domain. The motions are restricted to vertical plane motions.

3.1 Coordinate System

Figure 3-1 illustrates the coordinate systems adopted in the present computational model.

A global fixed coordinate system has $x, y, z-$axes, with $x-$axis lying in the undisturbed free surface, positive in the direction of forward velocity of the craft and $z-$axis positive downwards.

A body fixed coordinate system has $\xi, \chi, \zeta-$axes, originating at the centre of gravity (CG) of the craft, with $\xi-$axis positive in the direction of motion and $\zeta-$axis positive downwards.

The rotational pitch motion (θ) and mean trim (τ) are defined as positive for a bow-up condition.

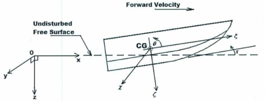

Figure 3-1: Coordinate system

3.2 Equations of Motion

Assuming the vessel acts as a rigid body, applying Newton's second law of motion:

$$M\ddot{x} = \sum F_X$$

$$M\ddot{z} = \sum F_Z$$

$$I\ddot{\theta} = \sum F_\theta \tag{3.1}$$

The generalized forces and moments on the right hand side of equation (3.1) can be separated into the specific components. Figure 3-2 illustrates the equilibrium of forces.

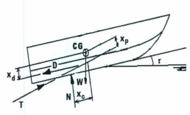

Figure 3-2: Equilibrium of forces

Considering the motions in the vertical plane of the craft, the motions are restricted to surge (x_{CG}), heave (z_{CG}) and pitch (θ). The equations of motion can be written as,

$$M\ddot{x}_{CG} = T_x - N\sin\theta - D\cos\theta = T_x + F_X - D\cos\theta$$

$$M\ddot{z}_{CG} = -T_z - N\cos\theta + D\sin\theta + W = -T_z + F_Z + D\sin\theta + W$$

$$I\ddot{\theta} = Nx_c - Dx_d + Tx_p = Tx_p + F_\theta - Dx_d \tag{3.2}$$

where M is mass of craft

I is pitch moment of inertia of craft

N is hydrodynamic normal force

D is friction drag

W is weight of craft

T_x is thrust component in x direction

T_z is thrust component in z direction

x_c is distance from center of gravity (CG) to center of pressure for normal force

x_d is distance from CG to center of action for friction drag force

x_p is moment arm of thrust about CG

3.3 Linear Theory of Wave Excitation

In the present computational model, wave forces are obtained by neglecting diffraction forces (only Froude-Kryloff forces are considered). It is also assumed that the wave excitation is caused by instantaneous wetted surface and by the vertical component of the wave orbital

velocity at the surface w_z. The influence of the horizontal component of wave orbital velocity on both the horizontal and vertical motions is neglected, because this velocity is considered to be relatively small in comparison with the forward speed of the craft $\dot{x}_{CG}$.

The normal velocity V and the velocity component parallel to the keel U can be written as functions of the craft's forward speed, heave, pitch and vertical component of wave orbital velocity.

$$U = \dot{x}_{CG}\cos\theta - (\dot{z}_{CG} - w_z)\sin\theta \quad (3.3)$$

$$V = \dot{x}_{CG}\sin\theta - \dot{\theta}\xi + (\dot{z}_{CG} - w_z)\cos\theta \quad (3.4)$$

For regular head waves, the wave elevation of a linear deep water wave,

$$\eta = \eta_0 \cos[k(x + ct)] = \eta_0 \cos(kx + \omega t) \quad (3.5)$$

where η_0 is the wave amplitude

k is the wave number

c is the wave celerity.

3.4 Sectional 2-D Hydrodynamic Force

The numerical model employed here for the prediction of vertical motions of a planing craft utilizes a strip theory with slender body approximations. The vessel is considered to be composed of a series of 2-D wedges and the three dimensional problem is subsequently solved as a summation of the individual 2-D slices.

The forces acting on a cross-section as demonstrated in Figure 3-3 consists of four components (force per unit length): the weight of the section (w), a hydrodynamic lift associated with the change of fluid momentum (f_M), a viscous lift force associated with the cross flow drag (f_{CD}) and a buoyancy force associated with instantaneous displaced volume (f_B).

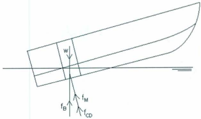

Figure 3-3: Forces acting on a section of a hull

The hydrodynamic lift force associated with the change of fluid momentum per unit length, f_M acting at a section is as follows,

$$f_M = \frac{D}{Dt}(m_a V) = m_a \dot{V} + V\dot{m}_a - \frac{\partial}{\partial \xi}(m_a V)\frac{d\xi}{dt}$$

$$= m_a \dot{V} + V\dot{m}_a - U\frac{\partial}{\partial \xi}(m_a V) \tag{3.6}$$

where m_a is the added mass associated with the section form

U is the relative fluid velocity parallel to the keel

V is the velocity in plane of the cross section normal to the baseline

The additional lift associated with the cross flow drag per unit length, f_{CD} is expressed as,

$$f_{CD} = C_D \rho b V^2 \tag{3.7}$$

where C_D is the cross flow drag coefficient

ρ is the density of the fluid

b is the half beam

The buoyancy force per unit length, f_B can be expressed as

$$f_B = a_{BF}\rho g A \tag{3.8}$$

where a_{BF} is the buoyancy correction factor

A is the cross sectional area of the section

The determination of all coefficients are described in section 3.8.

The flow over the hull is assumed to occur in transverse planes normal to the keel and not influenced by the cross-flow of other longitudinal positions. Two flow conditions exist, the chine's dry condition occurring near the leading edge of the wetted length of the craft

(Figure 3-4(a)) and a chine's wet condition occurring near the stern (Figure 3-4(b)). Sections between leading edge and stern oscillate between these two conditions.

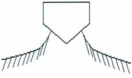

Figure 3-4(a): Cross-section flow condition: non-wetted chine

Figure 3-4(b): Cross-section flow condition: wetted chine

3.5 Slamming Force Estimation by Added-Mass Method

Added-mass is a widely used concept in a variety of applications like maneuvering, seakeeping and planing calculations. The amount of added mass varies according to the shape and size of the body. Payne (1988) gave added mass coefficients for many common body shapes, which were further investigated in details in Payne (1995).

The added mass for a V shaped wedge is given by,

$$m_a = k_a \frac{\pi}{2} \rho b^2 \tag{3.9}$$

$$\frac{dm_a}{dt} = \dot{m}_a = k_a \pi \rho b \dot{b} \tag{3.10}$$

where k_a is the added mass coefficient and b is the instantaneous half beam of the section.

Depth of penetration for each section is given by, $d = \dfrac{b}{\cot\beta}$

where β is the deadrise angle.

Taking into account the effect of water pileup, the effective depth of penetration (d_e) is expressed as,

$$d_e = C_{pu} d$$

where C_{pu} is the pile-up or splash up coefficient.

$$b = d_e \cot\beta = C_{pu} d \cot\beta \tag{3.11}$$

From (3.10), $\dot{m}_a = k_a \pi \rho b (C_{pu} \cot\beta) \dot{d}$ (3.12)

When the immersion exceeds the chine,

$$m_a = k_a \frac{\pi}{2} \rho b_{\max}^2 = \text{constant} \tag{3.13}$$

$$\dot{m}_a = 0$$

where $b_{\max}$ is the half beam at chine.

At any point P(ξ, ζ),

$$x = x_{CG} + \xi \cos\theta + \zeta \sin\theta \tag{3.14}$$

$$z = z_{CG} - \xi \sin\theta + \zeta \cos\theta \tag{3.15}$$

The submergence of a section in terms of the motion,

$$h = z - \eta$$

For wavelengths which are long in comparison to the draft and for small wave slopes, the immersion of a section measured perpendicular to the baseline is approximated as,

$$d = \frac{z-\eta}{\cos\theta - v\sin\theta} \tag{3.16}$$

where v is the wave slope.

The rate change of submergence is given by,

$$\dot{d} = \frac{\dot{z}-\dot{\eta}}{\cos\theta - v\sin\theta} + \frac{z-\eta}{(\cos\theta - v\sin\theta)^2} \cdot \frac{\partial(\cos\theta - v\sin\theta)}{\partial t}$$

Since the immersion $(z-\eta)$ is always small in the valid range, the relationship can be further simplified to

$$\dot{d} \approx \frac{\dot{z}-\dot{\eta}}{\cos\theta - v\sin\theta}$$

$$\dot{m}_a \approx k_a \pi\rho b(C_{pu}\cot\beta)\frac{\dot{z}-\dot{\eta}}{\cos\theta - v\sin\theta} \tag{3.17}$$

3.6 Total hydrodynamic force and moment

The total hydrodynamic forces acting on the vessel is obtained by integrating sectional 2-D forces over the wetted length l of the craft.

3.6.1 Vertical Direction (F_Z)

$$F_Z = \int_l f_M \cos\theta d\xi - \int_l f_{CD} \cos\theta d\xi - \int_l f_B d\xi$$

$$= -\int_l \left\{ m_a \dot{V} + V\dot{m}_a - U\frac{\partial}{\partial\xi}(m_a V) + C_D \rho b V^2 \right\} \cos\theta d\xi - \int_l a_{BF} \rho g A d\xi \tag{3.18}$$

For substitution,

$$\dot{V} = \ddot{x}_{CG}\sin\theta - \ddot{\theta}\xi + \ddot{z}_{CG}\cos\theta - \dot{w}_z\cos\theta + \dot{\theta}(\dot{x}_{CG}\cos\theta - \dot{z}_{CG}\sin\theta) + w_z\dot{\theta}\sin\theta \tag{i}$$

$$\frac{\partial U}{\partial \xi} = \frac{\partial w_z}{\partial \xi}\sin\theta \tag{ii}$$

$$\frac{\partial V}{\partial \xi} = -\dot{\theta} - \frac{\partial w_z}{\partial \xi}\cos\theta \tag{iii}$$

$$\frac{dw_z}{dt} = \dot{w}_z - U\frac{\partial w_z}{\partial \xi} \tag{iv}$$

$$\int u_1 dv_1 = u_1 v_1 - \int v_1 du_1 \tag{v}$$

Substituting the above equations into (3.18), we get,

$$F_Z = -\int_l \{[\ddot{x}_{CG}\sin\theta - \ddot{\theta}\xi + \ddot{z}_{CG}\cos\theta - \dot{w}_z\cos\theta + \dot{\theta}(\dot{x}_{CG}\cos\theta - \dot{z}_{CG}\sin\theta) + w_z\dot{\theta}\sin\theta]m_a$$

$$+ V\dot{m}_a - U\frac{\partial}{\partial \xi}(m_a V) + C_D\rho b V^2\}\cos\theta d\xi - \int_l a_{BF}\rho g A d\xi$$

$$= \{-\int_l m_a d\xi.\ddot{x}_{CG}\sin\theta + \ddot{\theta}\int_l m_a\xi d\xi - \int_l m_a d\xi.\ddot{z}_{CG}\cos\theta + \int_l m_a(\frac{dw_z}{dt} + U\frac{\partial w_z}{\partial \xi})\cos\theta d\xi$$

$$+ \int_l m_a d\xi\dot{\theta}(\dot{z}_{CG}\sin\theta - \dot{x}_{CG}\cos\theta) - \int_l m_a w_z\dot{\theta}\sin\theta d\xi - \int_l V\dot{m}_a d\xi + UV m_a\Big|_{bow}^{stern}$$

$$- \int_l m_a V\frac{\partial U}{\partial \xi}d\xi - \int_l C_D\rho b V^2 d\xi\}\cos\theta - \int_l a_{BF}\rho g A d\xi \tag{3.19}$$

Now putting $\int_l m_a d\xi = M_a$ and $\int_l m_a \xi d\xi = Q_a$ into equation (3.19), we get,

$$
\begin{aligned}
F_Z = \{ & -M_a \ddot{x}_{CG} \sin\theta + Q_a \ddot{\theta} - M_a \ddot{z}_{CG} \cos\theta + \int_l m_a \frac{dw_z}{dt} \cos\theta d\xi + \int_l m_a U \frac{\partial w_z}{\partial \xi} \cos\theta d\xi \\
& + M_a \dot{\theta}(\dot{z}_{CG} \sin\theta - \dot{x}_{CG} \cos\theta) - \int_l m_a w_z \dot{\theta} \sin\theta d\xi - \int_l V \dot{m}_a d\xi + UV m_a \Big|_{bow}^{stern} \\
& - \int_l m_a V \frac{\partial w_z}{\partial \xi} \sin\theta d\xi - \int_l C_D \rho b V^2 d\xi \} \cos\theta - \int_l a_{BF} \rho g A d\xi
\end{aligned}
\tag{3.20}
$$

3.6.2 Horizontal Direction (F_X)

The force acting in the horizontal x-direction is given by,

$$
\begin{aligned}
F_X &= -\int_l f_M \sin\theta d\xi - \int_l f_{CD} \sin\theta d\xi \\
&= -\int_l \left\{ m_a \dot{V} + V \dot{m}_a - U \frac{\partial}{\partial \xi}(m_a V) + C_D \rho b V^2 \right\} \sin\theta d\xi \\
&= -M_a \ddot{x}_{CG} \sin^2\theta + Q_a \ddot{\theta} \sin\theta - M_a \ddot{z}_{CG} \sin\theta \cos\theta + \int_l m_a \frac{dw_z}{dt} \sin\theta \cos\theta d\xi + \int_l m_a U \frac{\partial w_z}{\partial \xi} \sin\theta \cos\theta d\xi \\
&\quad + M_a \dot{\theta}(\dot{z}_{CG} \sin\theta - \dot{x}_{CG} \cos\theta) \sin\theta - \int_l m_a w_z \dot{\theta} \sin^2\theta d\xi - \int_l V \dot{m}_a \sin\theta d\xi + UV m_a \Big|_{bow}^{stern} \sin\theta \\
&\quad - \int_l m_a V \frac{\partial w_z}{\partial \xi} \sin^2\theta d\xi - \int_l C_D \rho b V^2 \sin\theta d\xi
\end{aligned}
\tag{3.21}
$$

3.6.3 Pitch Moment (F_θ)

The hydrodynamic moment is obtained in a similar manner by integrating over the wetted length the product of the normal force per unit length and the corresponding moment arm.

$$
\begin{aligned}
F_\theta &= \int_l f_M \xi d\xi + \int_l f_{CD} \xi d\xi + \int_l f_B \cos\theta \xi d\xi \\
&= \int_l [m_a \dot{V} + \dot{m}_a V - U \frac{\partial(m_a V)}{\partial \xi} + C_D \rho b V^2 + a_{BM} \rho g A \cos\theta] \xi d\xi \\
&= \int_l m_a \xi d\xi . \ddot{x}_{CG} \sin\theta - \ddot{\theta} \int_l m_a \xi^2 d\xi + \int_l m_a \xi d\xi . \ddot{z}_{CG} \cos\theta - \int_l m_a (\frac{dw_z}{dt} + U \frac{\partial w_z}{\partial \xi}) \cos\theta \xi d\xi \\
&\quad - \int_l m_a \xi d\xi \dot{\theta} (\dot{z}_{CG} \sin\theta - \dot{x}_{CG} \cos\theta) + \int_l m_a w_z \dot{\theta} \sin\theta \xi d\xi + \int_l V \dot{m}_a d\xi + \int_l C_D \rho b V^2 \xi d\xi \\
&\quad + \int_l a_{BM} \rho g A \cos\theta \xi d\xi - U V m_a \xi \Big|_{bow}^{stern} + \int_l m_a V \frac{\partial (U\xi)}{\partial \xi} d\xi \\
&= \int_l m_a \xi d\xi . \ddot{x}_{CG} \sin\theta - \ddot{\theta} \int_l m_a \xi^2 d\xi + \int_l m_a \xi d\xi . \ddot{z}_{CG} \cos\theta - \int_l m_a (\frac{dw_z}{dt} + U \frac{\partial w_z}{\partial \xi}) \cos\theta \xi d\xi \\
&\quad - \int_l m_a \xi d\xi \dot{\theta} (\dot{z}_{CG} \sin\theta - \dot{x}_{CG} \cos\theta) + \int_l m_a w_z \dot{\theta} \sin\theta \xi d\xi + \int_l V \dot{m}_a d\xi + \int_l C_D \rho b V^2 \xi d\xi \\
&\quad + \int_l a_{BM} \rho g A \cos\theta \xi d\xi + U V m_a \xi \Big|_{stern} + \int_l m_a V U d\xi + \int_l m_a V \frac{\partial U}{\partial \xi} \xi d\xi \\
&= Q_a \ddot{x}_{CG} \sin\theta - I_a \ddot{\theta} + Q_a \ddot{z}_{CG} \cos\theta - \int_l m_a \frac{dw_z}{dt} \cos\theta \xi d\xi - \int_l m_a U \frac{\partial w_z}{\partial \xi} \cos\theta \xi d\xi \\
&\quad - Q_a \dot{\theta} (\dot{z}_{CG} \sin\theta - \dot{x}_{CG} \cos\theta) + \int_l m_a w_z \dot{\theta} \sin\theta \xi d\xi + \int_l V \dot{m}_a \xi d\xi + \int_l C_D \rho b V^2 \xi d\xi \\
&\quad + \int_l a_{BM} \rho g A \cos\theta \xi d\xi + U V m_a \xi \Big|_{stern} + \int_l m_a V U d\xi + \int_l m_a V \frac{\partial w_z}{\partial \xi} \sin\theta \xi d\xi
\end{aligned}
\tag{3.22}
$$

where $\int_l m_a \xi d\xi = Q_a$

$\int_l m_a d\xi = M_a$

and $\int_l m_a \xi^2 d\xi = I_a$

3.7 Final Equations of Motion

Combining (3.20), (3.21) and (3.22), we get,

$$(M + M_a \sin^2\theta)\ddot{x}_{CG} + (M_a \sin\theta\cos\theta)\ddot{z}_{CG} - (Q_a \sin\theta)\ddot{\theta} = T_X + F_X' - D\cos\theta \qquad (3.23)$$

$$(M_a \sin\theta\cos\theta)\ddot{x}_{CG} + (M + M_a \cos^2\theta)\ddot{z}_{CG} - (Q_a \cos\theta)\ddot{\theta} = -T_Z + F_Z' + D\sin\theta + W \quad (3.24)$$

$$-(Q_a \sin\theta)\ddot{x}_{CG} - (Q_a \cos\theta)\ddot{z}_{CG} + (I + I_a)\ddot{\theta} = F_\theta' - Dx_d + Tx_p \qquad (3.25)$$

where $F_X' = F_X - \left\{-(M_a \sin^2\theta)\ddot{x}_{CG} - (M_a \sin\theta\cos\theta)\ddot{z}_{CG} + (Q_a \sin\theta)\ddot{\theta}\right\}$

$$F_Z' = F_Z - \{-(M_a \sin\theta\cos\theta)\ddot{x}_{CG} - (-M_a \cos^2\theta)\ddot{z}_{CG} + (Q_a \cos\theta)\ddot{\theta}\}$$

$$F_\theta' = F_\theta - \{(Q_a \sin\theta)\ddot{x}_{CG} + (Q_a \cos\theta)\ddot{z}_{CG} - I_a\ddot{\theta}\}$$

The mass matrix thus becomes,

$$A_{11} = M + M_a \sin^2\theta$$

$$A_{12} = M_a \sin\theta\cos\theta$$

$$A_{13} = -Q_a \sin\theta$$

$$A_{21} = A_{12} = M_a \sin\theta\cos\theta$$

$$A_{22} = M + M_a \cos^2\theta$$

$$A_{23} = -Q_a \cos\theta$$

$$A_{31} = A_{13} = -Q_a \sin\theta$$

$$A_{32} = A_{23} = -Q_a \cos\theta$$

$$A_{33} = I + I_a$$

The inverted matrix is then used to solve the following equations:

$$\ddot{x}_{CG} = A_{11}^{-1}F_1 + A_{12}^{-1}F_2 + A_{13}^{-1}F_3$$

$$\ddot{z}_{CG} = A_{21}^{-1}F_1 + A_{22}^{-1}F_2 + A_{23}^{-1}F_3$$

$$\ddot{\theta} = A_{31}^{-1}F_1 + A_{32}^{-1}F_2 + A_{33}^{-1}F_3 \qquad (3.26)$$

3.8 Determination of Coefficients ($k_a, a_{BF}, a_{BM}, C_{pu}, C_D$)

To compute the integrals of the total hydrodynamic forces and moments, the values of all these coefficients ($k_a, C_{pu}, C_D, a_{BF}, a_{BM}$) have to be determined.

Zarnick (1978) used $k_a = 1.0$ as the added mass coefficient, which is originally taken from Wagner (1932). Keuning (1994) in his model FASTSHIP and Payne (1995) in his model BOAT3D used an added mass coefficient which is dependent on the deadrise angle:

$$k_a = \left(1 - \frac{\beta}{2\pi}\right)^2 \qquad (3.27)$$

Akers (1999) used the following formula which is deadrise-dependent for his analysis:

$$k_a = \frac{\pi^2}{4}\left(1 - \frac{\beta}{90} \times 0.4 \times (1 - KAR)\right) \qquad (3.28)$$

where KAR is an added mass correction factor.

Hydrostatic forces and moments are very difficult to predict at planing speeds. Water splash up causes an increase in hydrostatic lift at the bow while flow separation decreases the hydrostatic lift at the stern, and both cause an increase in pitching moment. Zarnick

(1978) used $a_{BF} = 0.5$ for buoyancy correction following Shuford (1958) and $a_{BM} = 0.5a_{BF}$ for moment correction to achieve an accurate trim angle.

Keuning (1994) found Zarnick's constant values are only applicable for very high speeds. He approximated the sinkage and trim of the craft under consideration using polynomial expressions derived from model test results. Since the solution of the motion equations were known, substitution of the values of sinkage and trim in the equations of motion resulted in a system of two equations with three unknowns. Assuming no additional correction for moment ($a_{BM} = 1.0$), the values of k_a and a_{BF} can now be determined [van Dayzen (2008)].

Payne (1995) used the term "dynamic suction" to describe the loss of buoyancy which occurs at the transom of the boat when it accelerates from rest. In the technical paper of BOAT3D [Singleton (2008)], it is mentioned that dynamic suction adjustment magnitude is decided by empirical means.

Akers (1999) mentioned that these coefficients can be set to 0.5 according to Shuford (1958) and Zarnick (1978), or they can be set empirically so that simulation results match tank test results. He showed both results, one using Zarnick's (1978) values termed as "low buoyancy" and another with coefficients to reproduce Fridsma's (1969) calm water resistance and trim.

For the splash up, the work of Wagner (1932) still contains the most used and referred analytical results. Wagner approximated the flow around the falling wedge to the known solution of a plate in a uniform flow. By letting the plate expand as a function of time the increasing wetted surface of the immersing wedge was modeled. The approach is often referred to as the expanding plate theory and is a formulation for infinitely small deadrise although Wagner suggests and exemplifies applications for deadrise in a range applicable to the planing hull. The local surface deformation according to Wagner becomes $C_{pu} = \pi/2$ regardless of the deadrise angle. In fact the pile-up is deadrise dependent and the $\pi/2$ suggested by Wagner is usually considered as an upper limit. Zhao and Faltinsen (1992) also showed that the pile-up factor varies from 1 to $\pi/2$ for deadrise angles of 90^0 to 0^0.

Zarnick (1978) used the value $C_{pu} = \pi/2$ following Wagner (1932). Keuning (1994) and Payne (1995) used the following expression for splash-up, which is originally from Pierson's hypothesis. They used the symbol ($1+\psi$) for splash-up.

$$1+\psi = \frac{\pi}{2} - \beta\left(1 - \frac{2}{\pi}\right) \tag{3.29}$$

In this case splash-up gives the desired properties,

$1+\psi = 1$, at $\beta = \dfrac{\pi}{2}$ (no splash-up) and

$1+\psi = \dfrac{\pi}{2}$, at $\beta = 0$ (upper limit)

Akers (1999) did not mention his splash-up factor.

For the cross flow drag coefficient (C_D), both Zarnick (1978) and Keuning (1994) followed the approach of Shuford (1958). In using Shuford approach, it is assumed that the cross flow drag coefficient for a V-section is equal to the drag of a flat plate corrected by the Bobyleff flow coefficient approximated by $\cos\beta$, i.e.

$$C_D = 1.0\cos\beta \tag{3.29}$$

Keuning (1994) used,

$$C_D = 1.33\cos\beta \tag{3.30}$$

The present computational model has options of changing these coeffiecients, but from an initial assessment, it is found that the coefficients used by Zarnick (1978) give the closest results overall. So, the coefficients used in the present thesis are as follows:

$$k_a = 1.0$$

$$a_{BF} = 0.5$$

$$a_{BM} = 0.5a_{BF}$$

$$C_{pu} = \frac{\pi}{2}$$

$$C_D = 1.0\cos\beta$$

3.9 Solution of Equations

The solution of the derived equations of motion is complicated. They form a set of three coupled second order non-linear differential equations which has to be solved using standard numerical techniques in the time domain. The set of equations is first transformed into a set of six coupled first order non-linear differential equations by introducing the following state vector $[x_1, x_2, x_3, x_4, x_5, x_6]$

where $x_1 = \dot{x}_{CG}$,

$x_2 = \dot{z}_{CG}$,

$x_3 = \dot{\theta}$,

$x_4 = x_{CG}$,

$x_5 = z_{CG}$,

$$x_6 = \theta. \tag{3.31}$$

The equations of motion now can be written as,

$$[A]\dot{\vec{x}} = \vec{F} \tag{3.32}$$

where $[A]$ = Mass matrix,

$\dot{\vec{x}}$ = State variable vector $= [x_1, x_2, x_3, x_4, x_5, x_6]$,

$\vec{F}$ = Force vector which itself function of state variables.

The solution of this set is found by,

$$\dot{\vec{x}} = [A]^{-1}\vec{F} \tag{3.33}$$

Where $[A]^{-1}$ = inverse of mass matrix.

The numerical method used to do the integration is the Runge-Kutta-Merson method. Knowing the initial state variables at time instant t_0, the equations are simultaneously solved for the small time increment Δt to yield the solution at $t_0 + \Delta t$.

3.10 Equations of Motion for the Simplified Case of Constant Speed

The surge degree of freedom can be decoupled since there is little effect on the pitch and heave motions [Martin (1978a), Fridsma (1969), Blake (2000)]. Also to compare with experimental results, the test conditions have to be such that the model is towed at constant forward speed. Hence the craft is assumed to travel at steady forward speed,

$\dot{x}_{CG} = \text{constant}$

It is also assumed that the thrust and drag forces are acting through the center of gravity (CG) and cancelling out each other. The equations of motion can now be simplified to,

$$\ddot{x}_{CG} = 0$$

$$(M + M_a \cos^2\theta)\ddot{z}_{CG} - (Q_a \cos\theta)\ddot{\theta} = F_Z' + W$$

$$-(Q_a \cos\theta)\ddot{z}_{CG} + (I + I_a)\ddot{\theta} = F_\theta' \qquad (3.34)$$

Chapter 4

Validation

A computer program PHMP (Planing Hull Motion Program) has been developed based on the mathematical formulation described in Chapter 3. The simulation results by PHMP are compared with the model test results of Fridsma (1969), Chiu & Fujino (1989) and Katayama et al. (2000) for validation.

4.1 Comparison with Fridsma (1969)

The first validation has been made against the experimental results of Fridsma (1969). He conducted experiments with a series of prismatic models [refer to Figure 4-1 and 4-2] at different speeds and different regular sea conditions.

The models tested were 3.75 ft long and had deadrise angles of 10, 20 and 30 degrees. The beam of the model was varied with length-beam ratios of 4, 5 and 6. The models were run at speed-length ratios of 2, 4, and 6 (corresponding beam Froude number, C_v=1.33, 2.66, and 4) with trim angles of 4 and 6 degrees and had displacements of 16 and 24 lbs. The wavelengths were varied with wavelength to boat length ratios of 1, 1.5, 2, 3, 4 and 5. The initial wave height was varied from 1 to 3 inches to check linearity and then was fixed at 1 inch for the other tests.

All the models compared here were 3.75 ft long and had a 0.75 ft beam with a displacement of 16 lb having initial trim angle of 4 degrees. Comparisons are in the speed regions of C_v =2.66 and 4. The test configurations had the following characteristics described in Table 4-1. The vertical centre of gravity (VCG) was constant at $0.294 * B$ above the keel for all models. The accelerations were measured at the longitudinal centre of gravity and at bow, 10% of the length aft of the stem.

Table 4-1: Model configurations from Fridsma (1969) used for comparison

Configuration	Deadrise, β (deg.)	Longitudinal centre of Gravity, LCG (%L)	Radius of Gyration, k (%L)	Beam Froude Number, C_v
A	20	59.0	25.1	2.66
B	20	62.0	25.5	4
I	10	59.5	25.0	2.66
J	10	68.0	26.2	4
K	30	61.0	24.7	2.66
M	30	60.5	24.8	4

Figures 4-3 and 4-4 show sample numerical results of the time histories of the heave and pitch motions of a typical case. The motions are periodic but not exactly sinusoidal.

Similar time histories for the bow and CG accelerations are shown in Figures 4-5 and 4-6. For comparison, the heave and pitch double amplitudes are obtained by averaging the crests and troughs of the ten consecutive cycles and summing the two figures. The double amplitude heave motions are non-dimensionalized by wave height and the double amplitude pitch motions by twice the wave slope. The maximum negative value of the acceleration has been used for the comparisons with the experimental results of Fridsma (1969).

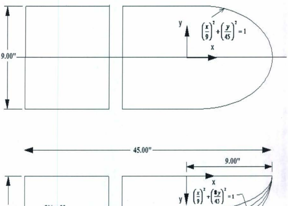

Figure 4-1: Keel profile and planform of prismatic models [Fridsma (1969)]

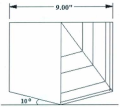

Figure 4-2: 10° deadrise model [Fridsma (1969)]

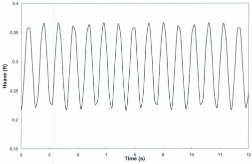

Figure 4-3: Sample time history of heave motion (20° deadrise model, $\lambda/L_{OA} = 4$, $H_w/B = 0.11$, $C_V = 4$)

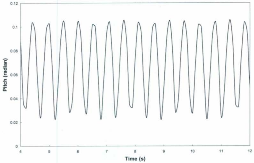

Figure 4-4: Sample time history of pitch motion (20° deadrise model, $\lambda/L_{OA} = 4, H_w/B = 0.11, C_V = 4$)

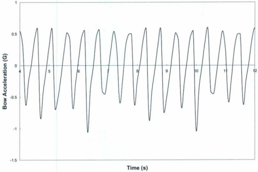

Figure 4-5: Sample time history of bow acceleration (20° deadrise model, $\lambda/L_{OA} = 4, H_w/B = 0.11, C_V = 4$)

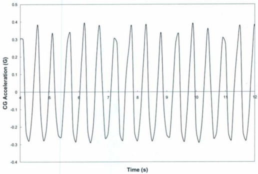

Figure 4-6: Sample time history of CG acceleration ($20°$ deadrise model, $\lambda/L_{OA} = 4, H_w/B = 0.11, C_V = 4$)

Figures 4-7 through to 4-12 show comparisons of the heave and pitch responses of the $10°$, $20°$ and $30°$ deadrise models running at C_v=2.66 and 4 respectively. In all cases the numerical model PHMP seems an accurate predictor of the motion amplitudes. The model can also predict accurately both the wavelength of the resonant frequency as well as the maximum amplitude of the motions. For the $10°$ deadrise, both heave and pitch motions show double resonant frequencies at C_v=4 as seen in Figures 4-7 and 4-10. Fridsma (1969) observed the model to rebound from a wave crest, to completely fly over a second wave crest and land again on the third. This pattern was found perfectly periodic and repeatable over many cycles. The numerical model PHMP predicts this double-resonant heave and pitch motions reasonably.

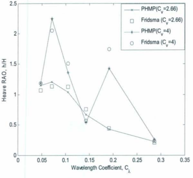

Figure 4-7: Heave response of the10° deadrise model

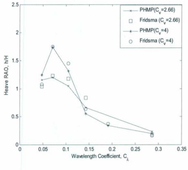

Figure 4-8: Heave response of the 20° deadrise model

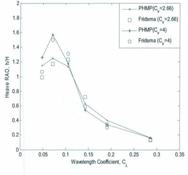

Figure 4-9: Heave response of the 30° deadrise model

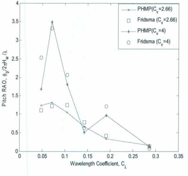

Figure 4-10: Pitch response of the 10° deadrise model

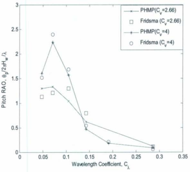

Figure 4-11: Pitch response of the 20° deadrise model

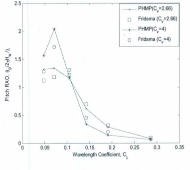

Figure 4-12: Pitch response of the 30° deadrise model

Bow and CG accelerations are very important design criteria for planing hulls. Figures 4-13 through to 4-18 show the bow and CG accelerations for the 10°, 20° and 30° deadrise models running at C_v=2.66 and 4 respectively. The simulated results by PHMP show reasonable accuracy in predicting those accelerations. However, the numerical model cannot reproduce the maximum amplitude of bow and CG accelerations for the 10° deadrise at C_v=4 as seen in Figures 4-13 and 4-16. To improve, the model needs to include exact slamming forces that occur at this speed with this smaller deadrise.

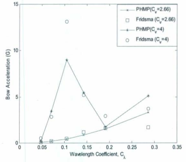

Figure 4-13: Bow acceleration of the 10° deadrise model

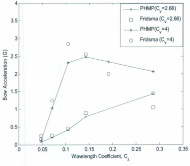

Figure 4-14: Bow acceleration of the 20° deadrise model

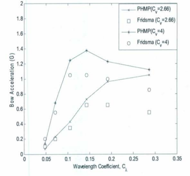

Figure 4-15: Bow acceleration of the 30° deadrise model

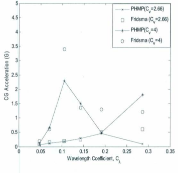

Figure 4-16: CG acceleration of the10° deadrise model

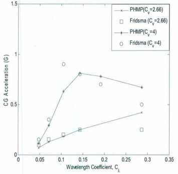

Figure 4-17: CG acceleration of the 20° deadrise model

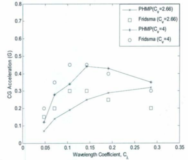

Figure 4-18: CG acceleration of the 30° deadrise model

4.2 Comparison with Chiu & Fujino (1989)

Chiu & Fujino (1989) used model test results to verify their numerical model. From their paper, some relevant results have been extracted to compare with the simulation results of PHMP. The simplified ship model of hard chine type, whose principal particulars and body plan are shown in Table 4-2 and Figure 4-19 respectively, is used. The model has uniform transverse sections from the transom to the square station no. $7\frac{1}{2}$. Chiu & Fujino (1989) measured the heave and pitch motions by potentiometers at the centre of gravity of the model. The initial sinkage (heave) and trim (pitch) were measured by running the model in calm water. They carried out the experiments in four different speed regimes of C_v = 0.0, 0.714, 1.429 and 2.143, termed as the stationary, non-planing, semi-planing and full-planing conditions, respectively.

Only the semi-planing (C_v=1.429) and full-planing (C_v=2.143) conditions have been used here for comparison.

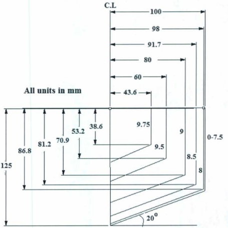

Figure 4-19: Body plan of the simplified ship model [Chiu & Fujino (1989)]

Table 4-2: Principal particulars of the simplified ship model [Chiu & Fujino (1989)]

Length , L_{OA}	0.8 m
Breadth, B	0.2 m
Depth, D	0.125 m
Transom draft, d	0.07 m
Deadrise angle, β	20°
Ship mass, m	5.054 kg
LCG from transom	0.296 m
VCG above keel	0.075 m
Initial trim	2.5°
Longitudinal radius of gyration	25.3% L

Figures 4-20 through to 4-23 show the experimental results by Chiu & Fujino (1989) and the simulated results by PHMP for the heave and pitch responses at C_v=1.429 and C_v=2.143 for three wave heights (H_w= 2.5, 4 and 5 cm). The heave and pitch response at C_v=1.429 is overestimated by PHMP for longer wavelengths (C_λ= 0.4 ~ 0.8) as seen in Figures 4-20 and 4-21. The heave response is a little bit underestimated and the pitch response is a little overestimated for longer wavelengths (C_λ= 0.4 ~ 1) as seen in Figures 4-22 and 4-23, yet in reasonable agreement.

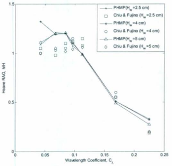

Figure 4-20: Heave Response of model at $C_v = 1.429$

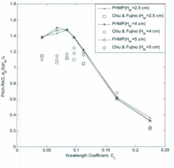

Figure 4-21: Pitch Response of model at $C_v = 1.429$

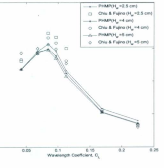

Figure 4-22: Heave Response of model at $C_v = 2.143$

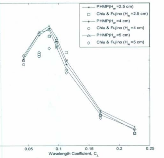

Figure 4-23: Pitch Response of model at $C_v = 2.143$

4.3 Comparison with Katayama et al. (2000)

Katayama et al. (2000) tested a model for much higher speed-length ratios compared with Fridsma (1969). Fridsma's speed-length ratios were 2, 4, and 6 knots per $ft^{1/2}$, whereas Katayama et al. (2000) published results for speed-length ratios of 4.1, 12.2, and 15.1 knots per $ft^{1/2}$. The model tests were carried out in the towing tank of Osaka Prefecture University and the model was a 1/4 scale model of a personal watercraft and its body plan is shown in Figure 4-24.

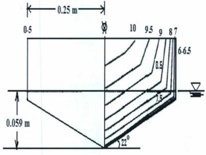

Figure 4-24: Body plan of the model of Jet-Ski [Katayama et. al (2000)]

The principal particulars of the model are shown in Table 4-3. They used a conventional 2 degrees of freedom arrangement and heave and pitch motions were measured by potentiometer. The radius of gyration was not published and it was assumed to be 25% of the model length during simulation.

Table 4-3: Principal particulars of the model of Jet-Ski [Katayama et. al. (2000)]

Length , L_{OA}	0.625 m
Breadth, B	0.250 m
Depth, D	0.106 m
Draft, d	0.059 m
Deadrise angle, β	22°
Ship weight, m	4.28 kg
LCG from transom	0.285 m
VCG above keel	0.111 m

Figures 4-25 and 4-26 show the heave and pitch motions with increasing wave height at waves of a single length $\lambda = 2.49L_{OA}$. At $C_v = 1.93$, the simulation results by PHMP for both heave and pitch underestimate the experimental results. At $C_v = 5.74$, the simulation results by PHMP tend to significantly underestimate the heave and pitch responses as wave height increases. At this very high speed range, huge hydrodynamic forces act on the planing hull and these are not modeled properly in the current simulation model. To improve this model, the slamming forces have to be replaced by accurate experimental results or by empirical prediction formula based on experimental results.

Figures 4-27 and 4-28 show the heave and pitch RAO with respect to wavelength at a single wave height $H_w = 0.68d$. At $C_v = 1.93$, the simulation results are still in fairly good agreement. At $C_v = 5.74$, the heave and pitch response produced by PHMP is very poor for short wavelengths ($\lambda/L_{OA} = 1.5 \sim 4.5$). A possible reason is that one of the assumptions of the current model is that wavelengths are large in comparison to boat length. That is why the simulation model cannot predict the responses accurately in this region.

Figures 4-29 and 4-30 show the heave and pitch RAO with respect to wavelength at $C_v = 5.74$ changing the wave height. At this very high speed the numerical model cannot predict the responses accurately and this effect increases with increasing wave height and for shorter wavelengths.

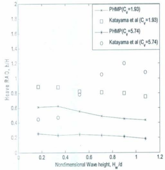

Figure 4-25: Heave response versus wave height at $\lambda/L_{OA} = 2.49$

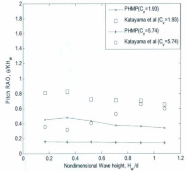

Figure 4-26: Pitch response versus wave height at $\lambda/L_{OA} = 2.49$

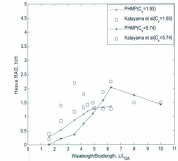

Figure 4-27: Heave response versus wavelength at $H_w = 0.68d$

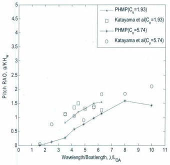

Figure 4-28: Pitch response versus wavelength at $H_w = 0.68d$

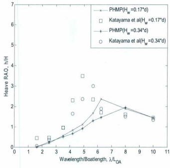

Figure 4-29: Heave response versus wavelength at $C_v = 5.74$

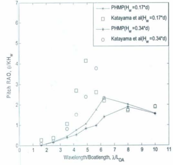

Figure 4-30: Pitch response versus wavelength at $C_v = 5.74$

The planing crafts jump out of the water and re-enters the incoming wave with significant slamming loads. This effect increases with increasing forward speed and wave height. PHMP cannot model the exact slamming loads at very high speeds and large wave conditions. For the accurate prediction of the motion amplitudes in such conditions, the slamming force should be predicted by more accurate empirical formulation based on experimental results in the current numerical model.

Chapter 5

Experimental Investigation

It has been found that the numerical model PHMP cannot simulate the motions exactly at the very high speed range due to inadequate modeling of slamming loads. Chuang (1973) developed a prediction method for determining slamming pressures of high speed vessels in waves. An experimental investigation has been carried out to get an accurate idea of two-dimensional impact loads and to verify Chuang's (1973) method for the simplified case of free fall drop tests with a 10° deadrise wedge.

5.1 The Experiment

The experiments were performed in the deep tank of the Ocean Engineering Research Center (OERC) at Memorial University of Newfoundland. Only vertical drop tests were conducted by varying the mass of the wedge and the drop height with the 10° deadrise model. The tests were conducted in calm water and the wind induced loading was negligible. The detail of the experimental setup is given in Mandeep et al. (2007); still the instrumentation and data acquisition system is briefly described here for better understanding.

5.1.1 Description of the experimental set-up

The frame (Figures 5-1(a) and 5-1(b)) used in the experiment was constructed using T-Slotted aluminum extrusions to get enough strength and rigidity and to facilitate easy disassembly of the frame when not in use. The frame was attached to the deep tank. The wedge apex was aligned perpendicular to the longitudinal axis of the tank.

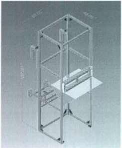

Figure 5-1(a): Front view of experimental frame with wedge attached to it [Mandeep et al. (2007)]

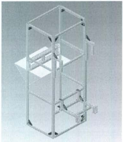

Figure 5-1(b): Back view of experimental frame with wedge attached to it [Mandeep et al. (2007)]

A trolley made of aluminum extrusions was used which slided on the guide rails fitted to the frame. The wedge was attached to the trolley and the guide rails provided high vertical drop speeds and high impact load bearing capacity. The linear motion guide rails were custom designed by Macron Dynamics Inc. [Mandeep et al. (2007)].

The 10° deadrise model (Figure 5-2) was made from 0.5 inch thick clear acrylic sheets. The wedge has been specifically designed to achieve rigidity and stiffness on impact and also to ensure that there is no ingress of water on the inside of the wedge. The wedge had a rectangular top on which attachments were fitted to vary the mass of the wedge.

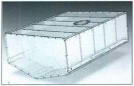

Fig.5-2: Design of 10° dead rise wedge [Mandeep et al. (2007)]

5.1.2 Instrumentation

A potentiometer cable extension transducer Celesco (PT5MA-150-S47-DN-500) with a range of 150 inches has been used along with two accelerometers (CTC Model AC140-2A) range 50g to measure the instantaneous vertical position and accelerations.

Four Piezoelectric pressure transducers (Kistler Model 211B4) were used to measure the pressure on the wedge surface. Their range is 0-200 psi and each of them has diameter of 5.5 mm. They were arranged along the median of the transducer attachment on one side of the wedge. Among the four pressure transducers, three of them were close to the apex and one was at the corner end of the side.

Two rectangular electromagnets (BRE-4080-110) of size 4" wide x 8" long x 2.5" high each manufactured by Bunting Magnetics Co. have been used so as to achieve remote automatic release of the trolley and wedge. The magnets have a rating of 1000 lbs for lifting application and are powered by 110 volts DC power supply (BPS1-0150-110).

5.1.3 Release mechanism

The Electro-magnets were fitted on the top of frame on underside of the cross-bar (Figure 5-3) and was electrically controlled to trigger the release of the trolley.

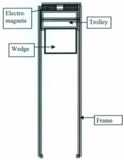

Figure 5-3: Trolley release mechanism [Mandeep et al. (2007)]

5.1.4 Data acquisition

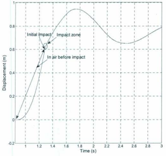

Figure 5-4: Displacement raw data as a function of time (No extra mass, drop height = 60 cm)

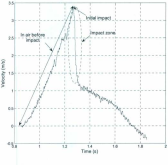

Figure 5-5: Wedge velocity as a function of time (No extra mass, drop height =60 cm)

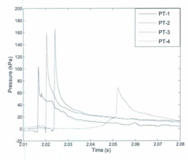

Figure 5-6: Recorded pressure by four pressure transducers during impact (Extra mass=20 kg, drop height =40 cm)

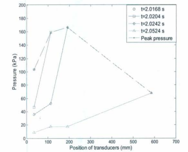

Figure 5-7: Pressure distribution on the face of the wedge at different times during impact (Extra mass=20 kg, drop height =40 cm)

at pressure transducer no.3 for all cases. The same conclusion can be drawn that the maximum pressure coefficient is independent of drop height, which was also observed by Yettou et al. (2005). The magnitude of the maximum pressure coefficient is also in the order of 80 as was found by the experimental results of Zhao et al (1996) and analytical results of Mei et al. (1999).

The maximum entry depth for the above cases corresponds to pressure transducer no. 3, which was the last transducer in contact with water at that instant. This maximum entry depth is also found remaining constant in the order of 1.5 as was reported by Yettou et al. (2005).

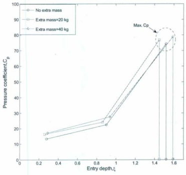

Figure 5-8: Effect of added mass on pressure coefficient as a function of dimensionless entry depth at drop height =40 cm

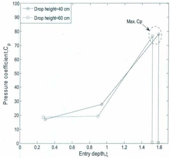

Figure 5-9: Effect of drop height on pressure coefficient as a function of dimensionless entry depth with added mass=40 kg

5.3 Comparison with Chuang's (1973) Prediction Method

Chuang (1973, 1976) developed a prediction method for determining slamming pressures of a high speed vessel in waves. This method is based on the Wagner wedge impact theory, the Chuang cone impact theory [Chuang (1969)] and NSRDC drop tests of wedges and cones.

According to this method, the pressure acting normal to the hull bottom in the slamming area may be separated into two components [Stavovy et al. (1976)]:

1. The impact pressure p_i, due to the normal component to the wave surface of the relative velocity between the impact surface and the wave.

2. The planing pressure p_p, due to the tangential component to the wave surface of the relative velocity between the impact surface and the wave.

The planing pressure is usually small and insignificant compared with the impact pressure. The total pressure due to normal velocity component of the vehicle both normal and tangent to the wave surface is therefore

$$p_t = p_i + p_p \tag{5.3}$$

In this thesis only the simplified case of wedge impact pressure in calm water is summarized. To estimate the maximum impact pressure, the pressure velocity relation is written as,

$$p_i = k\rho V_n^2 \tag{5.4}$$

where k is a non-dimensional coefficient, ρ is the mass density of water and V_n is the relative normal velocity of the impact body to the wave surface.

The relative normal velocity V_n is determined on the hypothesis that only the velocity component of the moving body normal to the impact surface and the velocity component of the wave normal to its surface generate the impact pressure [Stavovy et al. (1976)]. For the case of calm water impact, V_n becomes

$$V_n = V_v \cos^2 \beta \tag{5.5}$$

where V_v is the vertical impact velocity and β is the deadrise angle.

The non-dimensional coefficient, k is determined as follows,

$$k = k_1 / \cos^4 \beta \tag{5.6}$$

The best approximate values of k_1 are expressed by the following equation obtained through the method of curve fitting [Stavovy et al. (1976)]. For $2.2° \le \xi < 11°$:

$$k_1 = 2.1820894 - 0.9451815\xi + 0.2037541\xi^2 - 0.0233896\xi^3$$
$$+0.0013578\xi^4 - 0.00003132\xi^5 \quad (5.7)$$

where ξ is the impact angle which is equal to the deadrise angle β in the present case.

For all the cases of drop tests, pressures have been calculated using this method. It has been found that in each case, this method can predict the maximum pressure quite accurately for practical use which is summarized in Table 5-1.

Table 5-1: Comparison of maximum pressure with Chuang's (1973) prediction method

Configration	Maximum pressure [kPa] (Experimental result)	Maximum pressure [kPa] (Chuang's (1973) method)
No extra mass, 40 cm drop height	151.84	150.49
No extra mass, 60 cm drop height	280.64	268.49
20 kg extra mass, 40 cm drop height	166.51	150.67
20 kg extra mass, 60 cm drop height	262.26	249.41
40 kg extra mass, 40 cm drop height	186.53	171.61
40 kg extra mass, 60 cm drop height	268.64	265.29

Figures 5-10 through 5-12 show the comparison of recorded pressure with Chuang's (1973) prediction method for three cases. It is evident that Chuang's (1973) method can predict the maximum pressure almost exactly, provided that the vertical impact velocity is accurate. The main reason of the discrepancy of the results is due to the dynamic noise. Since the velocity is obtained by filtering the raw signal of displacement data and then differentiating them, the vertical impact velocity as an input was not perfectly accurate. This also caused a little bit time delay in predicting the maximum pressure.

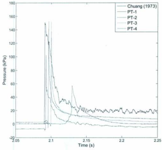

Figure 5-10: Comparison of recorded pressure with Chuang's (1973) prediction method

(No extra mass, drop height =40 cm)

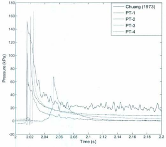

Figure 5-11: Comparison of recorded pressure with Chuang's (1973) prediction method

(Extra mass=20 kg, drop height 40cm)

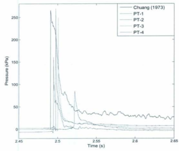

Figure 5-12: Comparison of recorded pressure with Chuang's (1973) prediction method

(Extra mass=40 kg, drop height =60 cm)

From the experimental results, it is evident that Chuang's (1973) prediction method is an accurate predictor of maximum slamming loads, though dynamic noise caused some discrepancies. More experiments need to be performed to investigate the effect of deadrise angle of the wedge. Oblique drop tests also need to be carried out in order to consider the motion in oblique waves. Further this method could be incorporated in the simulation of planing hull motion.

Chapter 6

Conclusions

6.1 Concluding Remarks

The problem of predicting the motion of high speed planing crafts is extremely difficult. The planing hull motions in waves lead to strong non-linearities that cannot be depicted well by linear analysis of motion. A non-linear mathematical model has been developed for predicting the vertical motions of a planing hull in regular head waves. Since the model is non-linear, the computations are made in the time domain. The model has its origins in the non-linear strip theory developed by Zarnick (1978). The model can input variable deadrise angles to account for different hull geometry. The numerical model is verified with the experimental model test results of Fridsma (1969), Chiu & Fujino (1989), and Katayama et al. (2000). The model has shown promising results in predicting the heave and pitch motions in semi-planing and planing regions of speed. For the super high speed vessels and to predict the vertical accelerations, the model still needs to include exact slamming forces.

An initial series of free fall drop tests have been performed with a $10°$ deadrise wedge varying the drop heights and the mass of the wedge. For each configuration, the maximum peak pressure was found in either pressure transducer number 2 or 3, which signifies that the peak pressure tends to increase from keel towards the chine. There was a big gap in space between pressure transducers number 3 and 4. This should be covered with more pressure transducers in the next experiments to depict a more accurate and complete spatial pressure distribution. The maximum pressure coefficient for this 10° model was found to be fairly constant at 80 and did not depend on drop heights and mass of the wedge. Chuang's (1973) prediction method has been found to predict maximum slamming loads quite accurately for each case, though dynamic noise caused some discrepancies.

6.2 Recommendation and Future Work

To improve the fidelity of the current algorithm, the following future work is recommended.

6.2.1 Experimental work

- Follow up experiments should be performed varying the deadrise of the wedge.
- Some oblique drop tests also need to be performed to get insight into the slamming phenomenon more accurately.
- Finally, model tests need to be carried out with a planing hull in waves to further verify Chuang's (1973) method. Then this method could be used to estimate the slamming loads of high speed vessels.

6.2.2 Numerical work

- To include Chuang's (1973) prediction method in the existing code PHMP to properly model slamming loads in waves.
- To include complicated ship geometry including variable deadrise angles, lifting strakes, spray rails etc. as far as possible to model more accurately the physical hull surface.
- To improve the estimates of hydrodynamic coefficients ($k_a, a_{BF}, a_{BM}, C_{pu}, C_D$) and to match a more efficient combination of these coefficients using Response Surface Methodology (RSM) to get a better approximation of motion data.
- To include freedom to surge and to add components of propulsion.
- To determine the added resistance in waves.
- To extend the current work for the case of irregular waves.

References

Akers, R. H. (1999): "Dynamic Analysis of Planing Hulls in the Vertical Plane", Ship Motion Associates, Portland, Maine, presented in the meeting of the New England Section of The Society of Naval Architects and Marine Engineers.

Akers, R., Hoeckley, S., Peterson, R., Troesch, A. (1999): "Predicted vs. Measured Vertical-Plane Dynamics of a Planing Boat." Proceedings: FAST'99, Seattle, USA. pp. 91-105.

Blake J.I.R. (2000): "Investigation into the Vertical Motions of High Speed Planing Craft in Calm Water and in Waves", PhD Dissertation, University of Southampton.

Breder, J. (2005): "Experimental Testing of Slamming Pressure on a Rigid Marine Panel", Master's Thesis, Naval Systems KTH Aeronautical and Vehicle Engineering, Stockholm, Sweden.

Caponnetto M., Azcueta R., Soding H. (2003): "Motion Simulations for Planing Boats in Waves", Ship Technology Research, Schiffstechnik, Vol 50, No. 4.

Chiu, Forng-chen., Fujino,M. (1989): "Nonlinear Prediction of Vertical Motions and Wave Loads of High-Speed Crafts in Head Sea", International Shipbuilding Progress, Vol. 36, No. 406, pp. 193-232.

Chuang, S.L. (1967): "Experiments on Slamming of Wedge-Shaped Bodies", Journal of Ship Research, Vol. 11, No. 3, pp. 190-198.

Chuang, S.L. (1973): "Slamming Tests of Three-dimensional Models in Calm water and Waves", NSRDC report 4095.

Clement, E.P. and Blount, D.L. (1963): "Resistance Tests of Systematic Series of Planing Hull Forms", SNAME Transactions 71, pp. 491–579.

Doctors, L.J. (1975): "Representation of Three Dimensional Planing Surfaces by Finite Elements", Proceedings of the 1st Conference on Numerical Ship Hydrodynamics, pp. 517–537.

Engle, A., Lewis, R. (2003): "A Comparison of Hydrodynamic Impacts Prediction Methods with Two-dimensional Drop Test Data" Marine Structures 16, pp. 175–182.

Faltinsen, O.M. (2005): "Hydrodynamics of High-Speed Marine Vehicles", Cambridge University Press, New York.

Fridsma, Gerard. (1969): "A Systematic Study of the Rough-Water Performance of Planing Boats", Report 1275, Davidson Laboratory, Stevens Institute of Technology, Hoboken, New Jersey.

Fridsma, Gerard. (1971): "A Systematic Study of the Rough Water Performance of Planing Boats (Irregular Waves -- Part II)", Report 11495, Davidson Laboratory, Stevens Institute of Technology, Hoboken, New Jersey.

Ghassemi, H., Yu-min, Su (2008): "Determining the Hydrodynamic Forces on a Planing Hull in Steady Motion", Journal of Marine Science and Application, Vol. 7, No. 3, pp. 147-156.

Grame, Karl, Rosén, A. (2003): "Time-Domain Simulations and Full-Scale Trials on Planing Craft in Waves", International Shipbuilding Progress, Vol. 50, No. 3, pp. 177-208.

Grame, Karl. (2004): "Modeling of Planing Craft in Waves", PhD thesis, Royal Institute of Technology KTH, Department of Aeronautical and Vehicle Engineering, Stockholm, Sweden.

Grame, Karl. (2005): "Improved Time Domain Simulation of Planing Hulls in Waves by Correction of the Near-Transom Lift", International Shipbuilding Progress, Vol. 52, No. 3, pp. 201-230.

Hicks, J.D., Troesch, A.W. and Jiang, C. (1995): "Simulation and Nonlinear Dynamics Analysis of Planing Hulls", Journal of Offshore Mechanics and Arctic Engineering, Vol. 117, No. 1, pp. 38-45.

Katayama, Toru, Hinami, Takashige and Ikeda, Yoshiho. (2000): "Longitudinal Motion of a Super High-Speed Planing Craft in Regular Head Waves", Proc. of the 4th Osaka Colloquium on Seakeeping Performance of Ships, pp. 214-220.

Keuning J. A. (1994): "The Nonlinear Behaviour of Fast Monohulls in Head Waves", Phd Thesis, Technische Universiteit Delft.

Lai, C., Troesch, A. (1995): "Modeling Issues Related to the Hydrodynamics of Three-Dimensional Steady Planing", Journal of Ship Research, Vol. 39, No. 1, pp. 1-24.

Lai, C., Troesch, A. (1996): "A Vortex Lattice Method for High Speed Planing", International Journal of Numerical Method in Fluids, Vol. 22, No. 6, pp. 495-513.

Lewis, S.G., Hudson, D.A., Turnock, S. R., Blake, J.I.R. & Shenoi, R. A. (2006): "Predicting Motions of High Speed RIBs: A Comparison of Non-linear Strip Theory with Experiments", Proceedings of the 5th International Conference on High Performance Marine Vehicles (HIPER'06), pp 210-224.

Mandeep, S.P., Qui, W., Veitch, B. (2007): "Experimental Design and Plan for Determining Slamming Loads", Proceedings of 8th Canadian Marine Hydromechanics and Structures Conference, St. John's, NL, Canada.

Martin M. (1978a): "Theoretical Determination of Porpoising Instability of High-Speed Planing Boats", Journal of Ship Research, Vol. 22, No. 1, pp. 32-53.

Martin M. (1978b): "Theoretical Prediction of Motions of High-Speed Planing Boats in Waves", Journal of Ship Research, Vol. 22, No. 3, pp. 140-169.

Mei, X., Lui, Y., Yue, D.K.P. (1999): "On the Water Impact of General Two-dimensional Sections", Applied Ocean Research 21, pp. 1-15.

Payne, P. R. (1981): "The Vertical Impact of a Wedge on a Fluid", Ocean Engineering, Vol. 8, No. 4, pp. 421-436.

Payne, P.R. (1982): "Contributions to the Virtual Mass Theory of Hydrodynamic Planing", Ocean Engineering, Vol. 9, No. 6, pp. 515-545.

Payne, P.R. (1988): "Design of High-speed Boats", Volume 1: Planing. Fishergate, Inc., Annapolis, Maryland, U.S.A.

Payne, P.R. (1994): "Recent Developments in 'Added-Mass' Planing Theory", Ocean Engineering, Vol. 21, No. 3, pp. 257-309.

Payne P. R., (1995): "Contributions to Planing Theory", Ocean Engineering, Vol. 22, No.7, pp. 699-729.

Payne, P.R. (1995): "A General Purpose Time Domain Program for High Speed Small Craft", Int. Conference Computer Aided Design & Production for Small Craft (CADAP'95).

Peseux, B., Gornet, L., Donguy, B. (2003): "Hydrodynamic Impact: Numerical and Experimental Investigations", Journal of Fluids and Structures 21, pp. 277-303.

Peterson, R., Wyman, D., Frank, C. (1997): "Drop Tests to support Water-impact and Planing Boad Dynamics Theory", Report No. CSS/TR-97/25, CSSDD NSWC, Panama City, Florida.

Savitsky, D. (1964): "Hydrodynamic Design of Planing Hulls", Marine Technology, Vol. 1, No. 1, pp. 71-95.

Savitsky, D. (1968): "On the Seakeeping of Planing Monohulls", Marine Technology, Vol. 5, No. 2, pp. 164-174.

Savitsky, D., Brown, P.W. (1976): "Procedures for Hydrodynamic Evaluation of Planing Hulls in Smooth and Rough Water", Marine Technology, Vol. 13, No. 4, pp. 381-400

Shuford, Charles L., Jr. (1958): "A Theoretical and Experimental Study of Planing Surfaces Including Effects of Cross Section and Plan Form", NACA Report 1355

Singleton, F. D. (2008): "Planing Boat Time-Domain Simulation with Waves", Digital Analytics, Houston, Texas, available online at: http://www.daoftx.com/b3dtechpaper.pdf

Spencer, Johns. (1975): "Structural Design of Crewboats", Marine Technology, Vol. 12, No. 3, pp. 267-274.

Stavovy, A.B., Chuang, S.L. (1976): "Analytical Determination of Slamming Pressures for High-Speed Vehicles in Waves", Journal of Ship Research, Vol. 20, No. 4, pp. 190-198.

Troesch, A.W. (1992): "On the Hydrodynamics of Vertically Oscillating Planing Hulls", Journal of Ship Research, Vol. 36, No. 4, pp. 317-331.

Thornhill, E., Oldford, D., Bose, N., Veitch, B. & Liu, P. (2001): "Planing Hull Model Tests for CFD Validation", 6th Canadian Marine Hydrodynamics and Structures Conference, Vancouver BC.

Tveitnes, T., Fairlie-Clarke, A.C., Varyani, K. (2008): "An Experimental Investigation into the Constant Velocity Water Entry of Wedge-shaped Sections", Ocean Engineering 35, pp. 1463-1478.

van Deyzen, Alex. (2008): "A Nonlinear Mathematical Model of Motions of a Planing Monohull in Head Seas", 6th international conference on high performance marine vehicles (HIPER'08).

Von Kármán, T. (1929): "The impact on seaplane floats during landing", Technical Notes, National Advisory Committee for Aeronautics.

Vorus, William S. (1996): "A Flat Cylinder Theory for Vessel Impact and Steady Planing Resistance", Journal of Ship Research, Vol. 40, No. 2, pp 89-106.

Wagner, H. (1936): "Phenomena Associated with Impacts and Sliding on Liquid Surfaces", translation of "Über stoß und gleitvorgänge an der oberfläche von flüssigkeiten, Zeitschrift Für Angewandte Mathematik Und Mechanik, 1932" NACA Library, Langley, Aeronautical Laboratory.

Wu, G.X., Sun, H., He, Y.S. (2004): "Numerical Simulation and Experimental Study of Water Entry of a Wedge in Free Fall Motion", Journal of Fluids and Structures 19, pp. 277-289.

Yettou, El-M., Desrochers, A., Champoux, Y. (2005): "Experimental Study on the Water Impact of a Symmetrical Wedge", Fluid Dynamics Research 38, pp. 47–66.

Zarnick E.E. (1978): "A Non-Linear Mathematical Model of Motions of a Planing Boat in Regular Waves", Technical Report. DTNSRDC-78/032, David Taylor Naval Ship Research and Development Center.

Zhao R., Faltinsen O. (1993): "Water Entry of Two-Dimensional Bodies", Journal of Fluid Mechanics", Vol. 246, pp. 593-612.

Zhao, R., Faltinsen, O.M., Aarsnes, J. (1996): "Water Entry of Arbitrary Two-dimensional Sections with and without Flow Separation", Proceedings of 21st Symposium on Naval Hydrodynamics, Trondheim, Norway.

Zhao, R., Faltinsen, O.M., & Haslum, H.A. (1997): "A Simplified Nonlinear Analysis of a High-Speed Planing Craft in Calm Water", 4th International Conference on Fast Sea Transportation (FAST'97).